

CrossMark
click for updatesCite this: *Catal. Sci. Technol.*, 2016,
6, 2560Received 30th November 2015,
Accepted 28th December 2015

DOI: 10.1039/c5cy02072g

www.rsc.org/catalysis

Mesopore incorporation into ZSM-5 enhances the dispersion of Pd nanoparticles throughout the hierarchical framework, significantly accelerating *m*-cresol conversion relative to a conventional microporous ZSM-5, and dramatically increasing selectivity towards the desired methylcyclohexane deoxygenated product. Increasing the acid site density further promotes *m*-cresol conversion and methylcyclohexane selectivity through efficient dehydration of the intermediate methylcyclohexanol.

Advances in the thermochemical processing of lignocellulosic biomass offer scalable routes to the production of sustainable liquid transportation biofuels from diverse waste-derived feedstocks.¹ Pyrolytic thermal decomposition of biomass delivers a broad product distribution, which varies with feedstock, reaction temperature and residence time.² Intermediate pyrolysis typically utilises low temperatures between 300–500 °C and long residence times which favour charcoal formation, whereas fast pyrolysis uses moderate temperatures of 450–550 °C and short vapour residence times <6 s to optimise liquid production. Higher temperatures and longer residence times favour gasification for direct power generation and upgrading of (purified) syngas *via* Fischer Tropsch and methanol synthesis. Of these routes, fast pyrolysis is the most promising for the direct conversion of agricultural waste and short rotation crops to bio-oils which retain up to 70% of the energy content of the raw biomass. Unfortunately, such fast pyrolysis bio-oils possess undesirable physicochemical properties including high oxygen contents of around 40 wt%, low pH, high viscosity and poor thermal stability, and relatively poor heating values of 16–19 MJ kg⁻¹, which hinders their use as drop-in

Hierarchical mesoporous Pd/ZSM-5 for the selective catalytic hydrodeoxygenation of *m*-cresol to methylcyclohexane†

James A. Hunns,^a Marta Arroyo,^b Adam F. Lee,^a José M. Escola,^b David Serrano^{*bc}
and Karen Wilson^{*a}

petroleum replacement fuels in conventional combustion engines.

A number of promising catalytic solutions to the upgrading of pyrolytic bio-oils are under development. Of these, solid acid (or base) catalysed esterification³ (or ketonisation) to ameliorate their low pH (arising principally from high acetic acid contents of 1–10%) through alkyl esters (or acetone) production, and subsequent hydrotreating to lower the oxygen content of ligneous and hemicellulosic depolymerisation products *via* hydrodeoxygenation (HDO),^{4,5} have proven most popular. HDO has been explored in batch and continuous upgrading mode, with early work utilising supported CoMo or NiMo sulfide catalysts^{6–8} analogous to hydrodesulfurization processes traditionally employed in petroleum refineries. Although such approaches permit oxygen removal, they are undesirable due to the requirement for H₂S in order to continuously regenerate the active sulfide phase. Transition metal catalysts have also been widely screened for HDO, affording significant deoxygenation, but under forcing conditions of high hydrogen pressures and process temperatures to deliver alkane products under batch and continuous processing.^{9–12}

Bifunctional transition metal-solid acid HDO catalysts are advantageous in combining a metallic component (usually Pt, Pd, Ni, Rh or Ru) to promote C=C and C=O hydrogenation, and an acid component to dehydrate aliphatic oxygenates (*e.g.* Al-SBA-15, ZSM-5 and beta zeolites, and sulfated metal oxides such as SO₄/ZrO₂). Consequently they permit lower hydrogen pressures than those required for direct hydrolysis over metal nanoparticles alone. However, the respective role of each active phase, and associated reaction mechanism and pathways, remains under debate.^{13–15} Hierarchical zeolites are a relatively new class of solid acids in which the incorporation of a second macroporous or mesoporous network may confer novel or improved catalytic performance. Mesoporous zeolites have previously shown activity for alkylation of benzene,¹⁶ conversion of methanol to hydrocarbons¹⁷ and other petrochemical cracking and isomerisation

^a European Bioenergy Research Institute, Aston University, Birmingham B4 7ET, UK. E-mail: k.wilson@aston.ac.uk; Tel: +44 (0)121 2044036

^b Chemical and Environmental Engineering Group, Rey Juan Carlos University, 28933, Móstoles, Madrid, Spain

^c IMDEA Energy Institute, 28935 Móstoles, Madrid, Spain.

E-mail: david.serrano@imdea.org

† Electronic supplementary information (ESI) available: Full synthetic, characterisation and reaction details. See DOI: 10.1039/c5cy02072g



processes.¹⁸ Mesopores in particular can improve accessibility to acid sites predominantly localised within the micropores of zeolites, thereby (at least partially) overcoming mass-transport limitations, which are especially important in the transformation of larger bio-derived reactants,¹⁹ and enhancing catalytic activity. Shorter diffusion lengths, and consequent in-pore residence times, may also influence product selectivity through the suppression of secondary reaction pathways. Hierarchical mesoporous zeolites may also be advantageous for improving the dispersion of promoters (e.g. metal nanoparticles) throughout the porous architecture, rather than their localisation on the external surface of conventional microporous counterparts.²⁰ Indeed, a Ni promoted, hierarchical nanocrystallite HBEA wide pore zeolite prepared *via* controllable base leaching was recently reported for stearic acid and palm oil hydrodeoxygenation which showed small improvements in stearic acid HDO selectivity to *n*-C₁₇/C₁₈ and iso-C₁₇/C₁₈ alkanes over microporous HBEA.²¹ Anisole HDO has also been performed over a hierarchical Ni/ZSM-5 catalyst,²² which exhibited high conversion and selectivity to cyclohexane.

Here we explore the impact of mesoporosity and acid strength upon *m*-cresol HDO over bifunctional, hierarchical Pd/ZSM-5 catalysts, which exhibit exceptional activity and selectivity towards the methylcyclohexane aliphatic product.

Hierarchical ZSM-5 zeolites were synthesised using the 'protozeolitic units silanization' method reported previously (ESI†).²³ Briefly, a solution of tetraethylorthosilicate, tetrapropylammonium hydroxide, aluminum isopropoxide (AIP) and deionized water was prepared to obtain Si:Al atomic ratios of 30 and 100, and pre-crystallization was induced under reflux prior to the addition of a seed silanization agent and extended hydrothermal aging. Samples are denoted as h-ZSM-5(*X*), where *X* is the theoretical Si:Al atomic ratio in the precursor gel. A commercial nanocrystalline ZSM-5 (Südchemie) was employed for comparison and denoted as c-ZSM-5(30). Zeolites were subsequently impregnated *via* incipient-wetness with 1 wt% palladium from PdCl₂, dried, calcined and reduced to yield Pd/h-ZSM-5(*X*) and Pd/c-ZSM-5(30). Bulk and surface physicochemical properties were characterized by elemental analysis, Ar porosimetry, powder XRD, and CO and NH₃ chemisorption to titrate metal and acid active sites, respectively. Hydrodeoxygenation was undertaken in a stirred batch autoclave employing 50 mg of catalyst and 6 mmol

m-cresol in *n*-dodecane at 200 °C and 20 bar H₂, with kinetic profiling *via* off-line GC analysis. Conversion and selectivity are reported ±2%, with the latter calculated for the three major liquid phase products 3-methylcyclohexanone (MCHO), 3-methylcyclohexanol (MCO), methylcyclohexane (MCX). Mass balances were between 90–99%.

Elemental analysis confirmed that the experimental Si:Al ratios were in good agreement with their nominal values (Table 1). BET surface areas of both hierarchical zeolites were higher than their conventional counterpart, increasing by 16% between c-ZSM-5(30) and h-ZSM-5(30), and further increased for the high silicon sample, mirroring the total pore volumes and secondary mesopore volumes (Table S1 and Fig. S1†). Wide angle XRD confirmed the presence of ZSM-5 crystallites in the commercial and hierarchical materials (Fig. 1), and showed that the introduction of mesoporosity had little impact on overall crystalline domain size. In contrast, mass normalised acid site densities from NH₃ chemisorption revealed that c-ZSM-5(30) possessed a slightly higher acid loading than h-ZSM-5(30) of 0.35 *versus* 0.3 mmol g⁻¹ respectively, whereas h-ZSM-5(100) possessed only one third of the acid sites. There was little difference in the maximum ammonia desorption peak temperatures between the three materials, indicating that varying the Si:Al ratio only influenced the number of acid sites, but not their strength (Table 1).

Pd impregnation resulted in similar metal loadings of ~1 wt% for all three zeolites, and was accompanied by a small decrease in surface area consistent with a small degree of pore blockage, but had negligible impact on the intrinsic zeolite acidity. The introduction of mesoporosity lowered the mean Pd nanoparticle size, an effect more significant for lower silicon (higher aluminium) content h-ZSM-5(30) material, a phenomenon previously observed for palladium impregnated silica and alumina.²⁴

Catalytic HDO of *m*-cresol proceeded efficiently over all three zeolites, with conversions varying between 78–100% achieved within 6 h reaction (Fig. 2). However, the acid site density and textural properties exerted a significant impact on the initial reaction rate. First considering the c-ZSM-5(30) and h-ZSM-5(30) catalysts, which exhibited very similar solid acid properties, mesopore incorporation doubled the rate of *m*-cresol HDO, although both catalysts attained full conversion within 6 h. We note that this rate enhancement did not directly correlate with the concomitant three-fold rise in

Table 1 Characterisation of bare and 1 wt% Pd impregnated ZSM-5 zeolites

Sample	Surface area ^a /m ² g ⁻¹	Pore volume ^a /cm ³ g ⁻¹	Si:Al atomic ratio	Zeolite crystal size ^b /nm	Pd particle size ^c /nm	Acid site density ^d /mmol g ⁻¹	T _{Max} NH ₃ ^d /°C
c-ZSM-5(30)	404	0.471	32	28	—	0.350	349
Pd/c-ZSM-5(30)	377	0.434	—	—	15.2	0.345	—
h-ZSM-5(30)	479	0.503	33	28	—	0.301	332
Pd/h-ZSM-5(30)	477	0.497	—	—	4.5	0.305	—
h-ZSM-5(100)	511	0.522	122	20	—	0.128	307
Pd/h-ZSM-5(100)	486	0.557	—	—	12.5	0.122	—

^a BET area from Ar physisorption. ^b Volume averaged crystallite domain size from XRD. ^c Mean diameter from CO chemisorption. ^d NH₃ TPD.



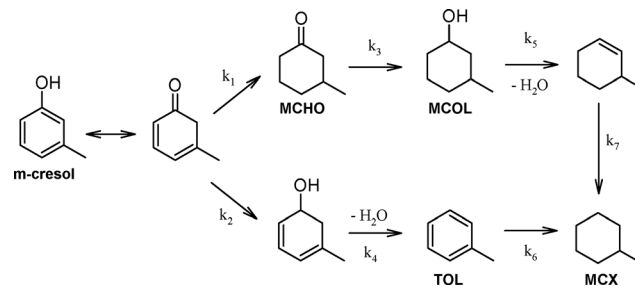


Fig. 1 Powder XRD patterns of conventional and hierarchical ZSM-5.



Fig. 2 *m*-Cresol conversion over conventional and hierarchical Pd/ZSM-5 catalysts.

palladium surface area (Table S1[†]), and hence is primarily attributed to improved mass transport and accessibility of in-pore acid sites. In contrast, increasing the silicon content



Scheme 1 Proposed reaction pathways for *m*-cresol HDO over Pd/ZSM-5 catalysts.

(lowering the acid site density from 0.31 to 0.12 mmol g⁻¹) resulted in a six-fold loss in activity for the h-ZSM-5(100) catalyst relative to h-ZSM-5(30); a high density of surface acid sites thus emerges as critical to efficient HDO under our conditions. The parent h-ZSM-5(100) material was inactive without palladium, confirming the requirement for metal centres to dissociatively adsorb hydrogen. However, there was no quantitative correlation between *m*-cresol HDO activity and the total palladium surface area. The metal surface area increased only three-fold between the Pd/h-ZSM-5(30) and Pd/h-ZSM-5(100) materials, far less than the corresponding rise in activity, evidencing a strong synergy between small Pd nanoparticles and strong acid sites.

All Pd/ZSM-5 catalysts yielded the same three liquid phase products MCHO, MCOL and MCX (Table 2). It has been previously proposed that *m*-cresol HDO over supported Pd and Pt (ref. 11–13) and Fe–Ni (ref. 25) proceeds *via* competitive alcohol deoxygenation *versus* ring hydrogenation (Scheme 1). However, in the present work, neither 3-methylcyclohexadienol nor toluene were observed, indicating that *m*-cresol HDO occurred exclusively *via* its tautomerisation to a cyclic dienone and subsequent ring hydrogenation to MCHO, which in turn underwent C=O hydrogenation and dehydration to MCX. The latter was observed as the dominant product at extended reaction times over the more acidic Pd/c-ZSM-5(30) and Pd/h-ZSM-5(30) catalysts, consistent with rapid dehydration of the MCOL intermediate, with the hierarchical variant achieving 99% MCX selectivity. It is interesting to note that kinetic profiling revealed ring hydrogenation to MCHO as the dominant pathway during the first hour of reaction (Fig. S2[†]), at which point the selectivity of the more acidic catalysts transitioned from favouring C=C hydrogenation to C=O hydrogenation. This switchover

Table 2 Activity and selectivity for *m*-cresol HDO over 1 wt% Pd/SZM-5 catalysts

Sample	Initial rate/mmol h ⁻¹ g _{Pd} ⁻¹	Selectivity ^a /%			
		MCX	TOL	MCHO	MCOL
Pd/c-ZSM-5(30)	17 143	66	0	31	3
Pd/h-ZSM-5(30)	35 750	99	0	1	0
Pd/h-ZSM-5(100)	6383	9	0	64	27

^a Reported at 6 h.



coincided with high levels of *m*-cresol conversion, and suggests slower C=O (of MCHO to MCOL) versus C=C hydrogenation, as commonly observed for unsaturated carbonyls over transition metals.²⁶ Interfacial interactions between metals and Lewis acid sites are reported to enhance C=O hydrogenation,²⁷ which may underpin the superior performance of the Pd/h-ZSM-5(30) versus Pd/h-ZSM-5(100) catalysts. We anticipate that the selectivity of Pd/c-ZSM-5 towards MCX will increase to mirror that of its hierarchical analogue at extended reaction times, reflecting the longer timescale for the former to achieve full *m*-cresol conversion. The less acidic Pd/h-ZSM-5(100) catalyst exhibited markedly different selectivity, favouring predominantly MCHO, accompanied by significant MCOL, as a consequence of its poorer activity for alcohol dehydration. The absence of the methylcyclohexene intermediate following MCOL dehydration demonstrates that alkene hydrogenation is rapid under these reaction conditions, as proposed for the stepwise transformation of related phenolics over Pd/zeolites. Further kinetic studies are currently underway to elucidate the rate-determining step in *m*-cresol HDO and the palladium structure sensitivity, in addition to the impact of palladium loading, H₂ pressure and the selection of phenolic substrate (e.g. *p*-cresol), in order to optimise the yield of cyclic alkanes and establish the generic applicability of hierarchical ZSM-5 in bio-oil HDO. In summary, mesopore introduction into a microporous zeolite significantly promotes the selective HDO of *m*-cresol to the desirable methylcyclohexane fully deoxygenated product.

Conclusions

Hierarchical ZSM-5 zeolites synthesised with intrinsic mesoporosity *via* crystallization of silanized protozeolitic units exhibit superior surface area and porosity over their purely microporous counterparts. These enhanced textural properties are attained without any change in the Si:Al composition, and with only a small loss in total acid site density. Mesoporosity increases the dispersion of palladium nanoparticles throughout a strongly acidic hierarchical zeolite, and in combination with associated improved mass transport, confers exceptional activity and selectivity for *m*-cresol HDO to methylcyclohexane *via* stepwise hydrogenation and dehydration. *m*-Cresol HDO occurs exclusively *via* its tautomerisation to a cyclic dienone and subsequent ring hydrogenation to MCHO over conventional and hierarchical Pd/ZSM-5 catalysts. A high density of acid sites is essential to ensure complete dehydration of 3-methylcyclohexanone and 3-methylcyclohexanol reactively formed hydrogenated intermediates. Tailoring the pore architecture of solid acids offers a facile means to improve the catalytic upgrading of bio-oils.

Acknowledgements

We thank the EPSRC (EP/K036548/1 and EP/K014706/1) for financial support. JAH thanks Johnson Matthey for an Industrial CASE studentship. KW thanks the Royal Society for an

Industry Fellowship. Support from the European Union Seventh Framework Programme (FP7/2007-2013) under grant agreement no. 604307 is also acknowledged.

Notes and references

- 1 A. V. Bridgwater, *Biomass Bioenergy*, 2012, **38**, 68–94.
- 2 W. N. R. W. Isahak, M. W. M. Hisham, M. A. Yarmo and T.-Y. Y. Hin, *Renewable Sustainable Energy Rev.*, 2012, **16**, 5910–5923.
- 3 L. Ciddor, J. A. Bennett, J. A. Hunns, K. Wilson and A. F. Lee, *J. Chem. Technol. Biotechnol.*, 2015, **90**, 780–795.
- 4 A. H. Zacher, M. V. Olarte, D. M. Santosa, D. C. Elliott and S. B. Jones, *Green Chem.*, 2014, **16**, 491–515.
- 5 Y. Wang, T. He, K. Liu, J. Wu and Y. Fang, *Bioresour. Technol.*, 2012, **108**, 280–284.
- 6 A. L. Jongorius, R. Jastrzebski, P. C. A. Bruijninx and B. M. Weckhuysen, *J. Catal.*, 2012, **285**, 315–323.
- 7 I. D. Mora, E. Mendez, L. J. Duarte and S. A. Giraldo, *Appl. Catal., A*, 2014, **474**, 59–68.
- 8 Y. Wang, H. Lin and Y. Zheng, *Catal. Sci. Technol.*, 2014, **4**, 109–119.
- 9 H. Ohta, H. Kobayashi, K. Hara and A. Fukuoka, *Chem. Commun.*, 2011, **47**, 12209–12211.
- 10 C. Newman, X. Zhou, B. Goundie, I. T. Ghampson, R. A. Pollock, Z. Ross, M. C. Wheeler, R. W. Meulenberg, R. N. Austin and B. G. Frederick, *Appl. Catal., A*, 2014, **477**, 64–74.
- 11 L. Nie and D. E. Resasco, *J. Catal.*, 2014, **317**, 22–29.
- 12 P. M. de Souza, L. Nie, L. E. P. Borges, F. B. Noronha and D. E. Resasco, *Catal. Lett.*, 2014, **144**, 2005–2011.
- 13 X. Zhu, L. Nie, L. L. Lobban, R. G. Mallinson and D. E. Resasco, *Energy Fuels*, 2014, **28**, 4104–4111.
- 14 X. Zhu, L. L. Lobban, R. G. Mallinson and D. E. Resasco, *J. Catal.*, 2011, **281**, 21–29.
- 15 J. Horacek, G. St'avova, V. Kelbichova and D. Kubicka, *Catal. Today*, 2013, **204**, 38–45.
- 16 H. Liu, S. Liu, S. Xie, C. Song, W. Xin and L. Xu, *Catal. Lett.*, 2015, **145**, 1972–1983.
- 17 Z. Liu, X. Dong, Y. Zhu, A.-H. Emwas, D. Zhang, Q. Tian and Y. Han, *ACS Catal.*, 2015, **5**, 5837–5845.
- 18 I. I. Ivanova, E. E. Knyazeva, A. A. Maerle and I. A. Kasyanov, *Kinet. Catal.*, 2015, **56**, 549–561.
- 19 H. W. Lee, B. R. Jun, H. Kim, D. H. Kim, J.-K. Jeon, S. H. Park, C. H. Ko, T.-W. Kim and Y.-K. Park, *Energy*, 2015, **81**, 33–40.
- 20 C. H. Christensen, I. Schmidt, A. Carlsson, K. Johannsen and K. Herbst, *J. Am. Chem. Soc.*, 2005, **127**, 8098–8102.
- 21 B. Ma and C. Zhao, *Green Chem.*, 2015, **17**, 1692–1701.
- 22 T. M. Sankaranarayanan, A. Berenguer, C. Ochoa-Hernández, I. Moreno, P. Jana, J. M. Coronado, D. P. Serrano and P. Pizarro, *Catal. Today*, 2015, **243**, 163–172.
- 23 D. P. Serrano, J. Aguado, J. M. Escola, A. Peral, G. Morales and E. Abella, *Catal. Today*, 2011, **168**, 86–95.
- 24 C. M. A. Parlett, L. J. Durndell, A. Machado, G. Cibin, D. W. Bruce, N. S. Hondow, K. Wilson and A. F. Lee, *Catal. Today*, 2014, **229**, 46–55.



- 25 L. Nie, P. M. de Souza, F. B. Noronha, W. An, T. Sooknoi and D. E. Resasco, *J. Mol. Catal. A: Chem.*, 2014, **388–389**, 47–55.
- 26 L. J. Durndell, C. M. A. Parlett, N. S. Hondow, M. A. Isaacs, K. Wilson and A. F. Lee, *Sci. Rep.*, 2015, **5**, 9425.
- 27 A. Y. Stakheev and L. M. Kustov, *Appl. Catal., A*, 1999, **188**, 3–35.

